Carbohydrate Polymers 105 (2014) 300–307

Contents lists available at ScienceDirect

Carbohydrate Polymers

journal homepage: www.elsevier.com/locate/carbpol

Properties and catalytic activity of magnetic and acidic ionic liquids: Experimental and molecular simulation

Cunshan Zhou[a,b,c,d], Xiaojie Yu[a], Haile Ma[a,b,c,*], Xingyi Huang[a], Henan Zhang[a], Jian Jin[a]

[a] School of Food and Biological Engineering, Jiangsu University, 301 Xuefu Road, Zhenjiang 212013, China
[b] Jiangsu Provincial Research Center of Bio-process and Separation Engineering of Agri-products, Jiangsu University, 301 Xuefu Road, Zhenjiang 212013, China
[c] Jiangsu Provincial Key Laboratory for Physical Processing of Agricultural Products, Jiangsu University, 301 Xuefu Road, Zhenjiang 212013, China
[d] Heddle Initiative Research Unit, Advanced Science Institute, RIKEN, 2-1 Hirosawa, Wako, Saitama 351-0198, Japan

ARTICLE INFO

Article history:
Received 22 November 2013
Received in revised form 14 January 2014
Accepted 21 January 2014
Available online 31 January 2014

Keywords:
Catalytic activity
Recyclability
Platform chemical
Dual functional ionic liquids
Molecular dynamics

ABSTRACT

The exploitation of dual functional magnetic and acidic ionic liquids (MAILs) for hydrolysis of cellulose to platform chemicals can solve some practical challenges through easy separation of products and efficient catalyst recyclability. In this work, seven $C_n$mim/$FeCl_4$ MAILs were synthesized and investigated with combined experimental and molecular dynamics. The MAILs contained $FeCl_4^-$ anions and exhibited a typical hard magnetic materials behavior with rather strong magnetic susceptibilities. These MAILs were stable up to 250–310 °C, the decomposition was started up at 250/310–480–810 °C in two steps with the formation of the undecomposed residue. The Gibbs energy for the reaction of glucose/xylose conversion to 5-hydroxymethylfurfural by metal chlorides in the $C_n$mimCl ionic liquid was studied using the density functional theory calculations and the results that C_3mim/WCl_3 may be the most hopeful catalyst. The MAILs have the potential to open up promising new catalytic systems because of their easy product separation and efficient catalyst recyclability.

1. Introduction

The exploitation and usage of fossil fuel is widely thought to be the cause of serious problems such as, climate anomalies (Friedlingstein & Solomon, 2005). Reserves of fossil fuels will eventually disappear and this will lead energy crisis (Shafiee & Topal, 2005). To prevent the imminent problems, alternative biofuels have been explored and successful stories such as first-generation biofuels from corn and soybean edible oil have confirmed the practical feasibility of biomass-to-biofuel (edible oil to gasoline) conversion. However, with the use of dependent survival agricultural and edible products and in this choice may create their own fatal problems such as food supply shortages as the world population grows and social issues (Godfray et al., 2010). Another option is typical and important chemical alternatives such as second-generation biofuels, feedstocks and platform chemicals produced from non-edible lignocellulosic biomass from agricultural waste (which has attracted most attention to date). Since considered and recognized as a particularly attractive option owing to its potential greener, and sustainability and carbon neutrality (Scheme 1) (Nel & Cooper, 2009). Until now, a great deal of work has been carried on the hydrolysis of cellulose with cellulases, mineral acids and solid acids. Enzymatic hydrolysis of cellulose is rather effective, but the reaction is sensitive to environmental contaminants, and suffers from inefficiency and a high enzyme cost (Engel et al., 2010; Salvador et al., 2010). Mineral acids have been comprehensively investigated to catalyze the degradation of cellulose at a variety of acid concentrations, high temperatures (180–250 °C) and high pressure. Furthermore, as far as safety and green concerned, degradation of the resulting glucose and some intermediates becomes an issue at such high temperatures. Meanwhile, large-scale use of mineral acid suffers from several related problems such as reactor corrosion, catalyst recovery/reuse and requires treatment of the waste, producing lots of pollution (Torget et al., 2000). The catalytic hydrolysis of cellulose into glucose with solid acids has the advantage of avoiding some of the above shortcoming owing to the ease of catalytic separation, recyclability and reduced damage to the corrosion (Shimizu & Satsum, 2011). Significant progress of this catalytic conversion has been made by using various types of particles acids with large pore size and super acid strength. As far as the real biomass feedstock and practical process for the hydrolysis of cellulose to glucose is concerned, challenges still exist for the solid acids catalytic system (Xu et al., 2011; Lange et al., 2012). Solid acids catalysts cannot be directly separated when residues are formed as solid power in the reaction process. Additionally, several important aspects also need to be looked at, and such as economic feasible, simplicity to

* Corresponding author. Tel.: +86 511 88790958; fax: +86 511 88780201.
E-mail address: mhl@ujs.edu.cn (H. Ma).

0144-8617/$ – see front matter © 2014 Elsevier Ltd. All rights reserved.
http://dx.doi.org/10.1016/j.carbpol.2014.01.071

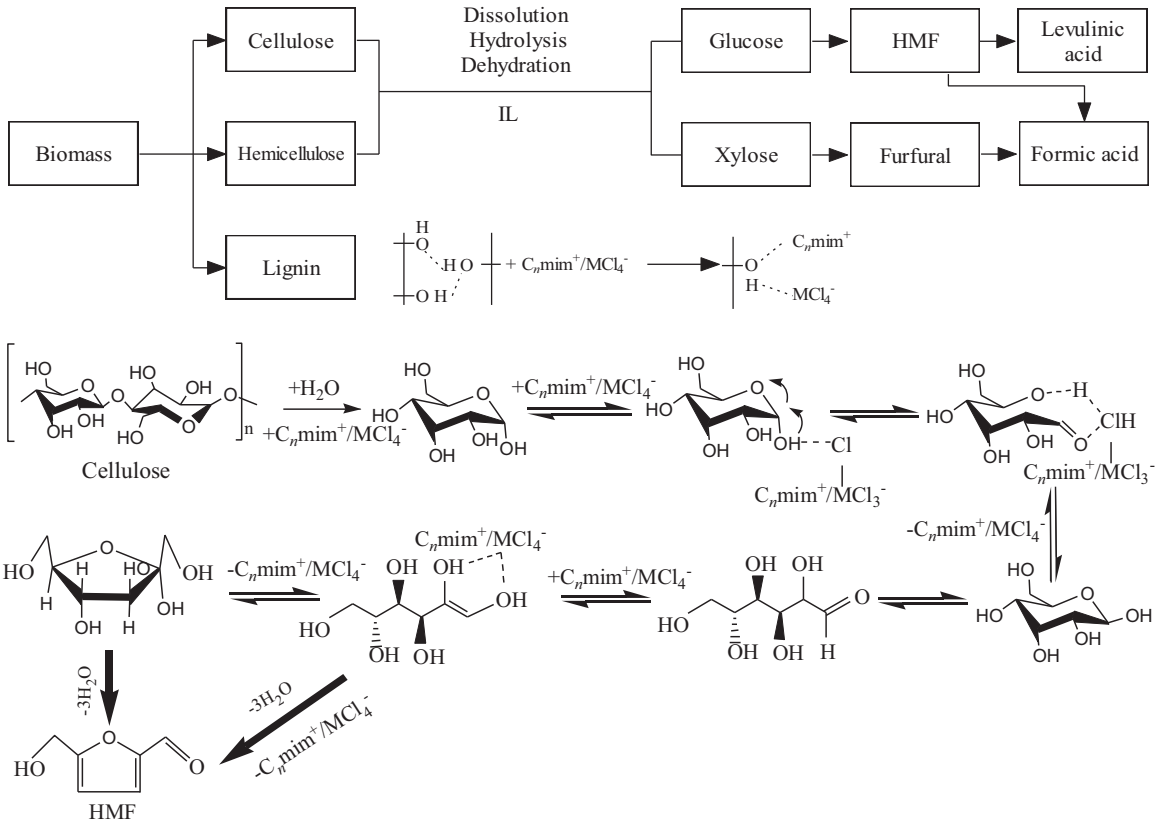

Scheme 1. Possible dissolution mechanism of cellulose in $C_n$mim/MCl_4 MAILs and conversion of cellulose to HMF catalyzed with $C_n$mim/MCl_4MAILs (n = 4, 6, 8, 10, 12, 14, 16).

enlarge, efficiency and environmental green (Huang & Fu, 2013). Overall, economic, environmental, and sustainable aspects should be of concern when designing new catalytic systems.

Ionic liquids (ILs) have gained enormous attention in the past 30 years. They are solvents and are often regarded as "green", "designable", "friendly", "non-coordinating" etc., nevertheless it is increasingly recognized that none of these tags could be used easily. Yet, considerable research in ILs green chemistry is still learned by trial-and-error method rather than fundamental principle of understanding and reasonable design. Not enough is known to date about properties and structures of these new materials in the liquid phase nor are all observed differences in reaction outcomes as compared to "conventional" solvents explained satisfactorily (Zhou, Yu, Ma, He, & Vittayapadung, 2013a; Zhou et al., 2013b). Recently, ILs have attracted more and more attention and have been utilized as catalysts for the hydrolysis of lignocellulosic biomass. The first mention of the dissolution of cellulose in an ILs was in 1934, but the utilization of ILs in the lignocellulose biofuel conversion only started from 2000 as a result of the energy crisis. In many of the possible biomass based chemicals, 5-hydroxymethylfurfural (HMF) is derived from dehydration of saccharides, such as pentose, hexoses, sucrose, cellulose and inulin, and is considered as a pivotal building block in biomass biorefinery because it can derive a variant of beneficial derivatives, including 2, 5-dimethylfuran, which is a hopeful biofuel, 2, 5-diformylfuran, 2, 5-furandicarbaldehyde and 2, 5-furandicarboxylic acid (Zakzeski et al., 2010). Catalytic dehydration of pentose (fructose) to HMF making use of both homogeneous and heterogeneous catalytic reaction systems has been investigated extensively (Nishiyama et al., 2002). Notwithstanding the conversion of fructose to HMF without catalysts, higher yields of HMF have been realized with many catalysts, such as ion-exchange resins, ionic liquids, zeolites, and metal halide. In 2007, Zhao et al. (Zhao, Holladay, Brown, & Zhang, 2007) discovered that $CrCl_2$ in [EMIM]Cl (1-ethyl-3-methylimidazolium chloride; an imidazolium type ionic liquid) can efficiently catalyze the conversion of glucose to HMF.

Despite all the researches carried out in this area, there is little explanation on the reaction mechanism for the glucose/fructose conversion to HMF. Especially, glucose/fructose degradation in ionic liquid/metal halide catalysts remains poorly understood mechanistically, although somewhat experimental results have confirmed the essential nature of Cr species and the coordination characteristics of the complex between metal salts and sugars (Hu et al., 2009). However, in a recent DFT computations combined with EXAFS study, a transient binuclear Cr(II) species was reported to be in charge of the glucose/fructose isomerization necessary step (Pidko, Degirmenci, van Santen, & Hensen, 2010).

Magnetic 1-butyl-3-methylimidazolium tetrachloroferrate (bmim/$FeCl_4$) was synthesized and first reported by Hayashi et al. (Hayashi, Saha, & Hamaguchi, 2006), but they did not mention the acidic property of the tested ILs at the same time in the paper. It would be extremely interesting and necessary to investigate the macroscopic and microscope responses of those multifunctional ionic liquids to a magnet in quantitative ways. Magnetic and acidic ionic liquids (MAILs) not only have the excellent properties of conventional ionic liquids, such as wide liquid range, higher ionic conductivity, excellent solubility, thermal stability and designability by appropriate modifications of cations or anions in structures, but also exhibit an unexpectedly strong response to an additional magnetic field and acidic catalytic activity. These properties make MAILs have more advantages and potential application prospects than conventional ILs in the fields of catalytic reactions (Wang et al., 2011; Misuka et al., 2011), solvent effects (Kim et al., 2008) and separation processes (Pei et al., 2010; Wang et al., 2010).

In this paper, seven $C_n$mim/$FeCl_4$ MAILs with the same imidazole cationic rings were synthesized and tested in a combined experimental and molecular dynamics simulation study, which has not previously been reported in the literature. The catalytic activity of the reaction of glucose and xylose conversion to HMF by metal chlorides (MCl_3, M=Cr, Fe, Mo, W) in $C_n$mimCl (n = 2,3,4) ionic liquid (Scheme 1) has been studied using DFT calculations. These studies will provide important and fundamental references for further synthesizing MAILs with stronger magnetism, and offer more chances for the usage of MAILs in utilization of lignocellulose and for the conversion of biomass to biofuel or derived chemicals challenging which can solve energy crisis in future.

2. Methods

2.1. Materials

N-Methylimidazole (≥99.0%), methanesulfonyl chloride (≥99.7%), triethyl amine (≥99.5%), diethylene glycol (≥99.0%), triethylene glycol (≥99.0%), tetra ethylene glycol (≥95.0%), $FeCl_3{\cdot}6H_2O$, pyridine, *n*-chlorobutane, acetonitrile and ethyl acetate were of analytical grade and were used without further purification.

2.2. Preparation of magnetic ionic liquids

In the present study, the preparation of MAILs (shown in Scheme 2), such as C_4mim/$FeCl_4$, was synthesized according to the following methods (Bourissou, Guerret, Gabbai, & Bertrand, 2000). Firstly, *N*-butylpyridiumchloride intermediates were prepared by reacting of 0.2 mol *N*-methylpyrrolidine with 0.24 mol *n*-chlorobutane at 80 °C for 48 h with magnetic stirring. The reaction intermediate products were purified and recrystallized from acetonitrile repeatedly, subsequently washed with ethyl acetate for four times and dried in a vacuum oven at 60 °C for 24 h. Secondly, the intermediates $C_n$mimCl were mixed with equimolar of $FeCl_3{\cdot}6H_2O$ under N_2 atmosphere with magnetic stirring at room temperature (~25 °C). The final products were washed with ether and deionized water repeatedly, purified by reduced pressure distillation and dried in a vacuum oven at 60 °C for 24 h successively. The MAILs, $C_n$mim/$FeCl_4$, were obtained for further experiments.

2.3. Characterization

Raman spectra were recorded by a microscopic confocal LabRAM HR-800 Raman spectroscopy (France, Jobin-Yvon) using a 532 nm laser (He–Ne 632.8 nm, Nd:YAG laser 532 nm) beam and an air-cooled charge-coupled detector (CCD) with 4 cm^{-1} resolution.

Fourier transform infrared spectroscopy (FTIR) spectra of the samples (as pellets in KBr) were recorded by a Thermo Electron Nicolet Nexus 670 FTIR spectrometer in a wavenumber range of 400–4000 cm^{-1} at a resolution of 4 cm^{-1}.

The ultraviolet and visible absorption spectrum (200–500 nm) was detected using a Hitachi U-3500 UV–vis spectrometer.

Thermo gravimetric analysis (TGA) was measured on a TG-DSC PerkinElemer Pyris Diamond thermal analyzer at a heating rate of 10 °C min^{-1} under N_2 atmosphere.

The magnetic susceptibilities of MAILs were carried out with a MPMS (SQUID) (America, Quantum Design).

2.4. Computational details

The coordination condition of the chromium center in the $[MMIM]^+$ (M = methyl) cation and $CrCl_3^-$ anion for ionic liquid [MMIM]/$CrCl_3$ was studied with the method of DFT (density functional theory) calculations (Pidko et al., 2010). In order to explain the complex influence of the type with different cations and anions in ILs on the catalyzed hydrolysis reaction, and to acquire molecular level mechanism of the exclusive efficiencies of chromium *N*-heterocyclic carbenes, a reduced model was put forward in this work. In the initial and preliminary geometry, the deprotonated [BMIM] (1-butyl-3-methylimidazolium) ligand was bound to $Cr^{III}Cl_3$ through the lone pair of electrons of the carbon atom which is located between two highly electronegative nitrogen atoms, resulting in the construction of a direct Cr—C bond and a tetrahedral Cr—Cl species. It is known that the structure of deprotonated [BMIM] ligand bears very similarity to the well-outlined *N*-heterocyclic carbenes that have been engaged to stabilize and maintain catalysts based on Cr and other elements of transition metals (Bourissou et al., 2000). Further more, the addition of glucose or other monosaccharides to the [BMIM]/$CrCl_3$ site comes into being six-coordinated Cr intermediates, which were often and easily found in the crystal structures of Cr (III) complexes.

DFT calculations were carried out using the B3LYP of nonlocal three-parameter density functional, which joins the Becke's exchange and Lee et al. (Lee et al., 1988) conjunction functionals (Hatakeyama et al., 2009).

The LANL2DZ bases fix with relativistic effective core potential (RECP) of Hay and Wadt (Hay & Wadt, 1985) was applied to describe the transition metal elements (Cr, Fe, Mo and W), and the 6–31 G + (d,p) for all the remaining elements (Liang et al., 2009).

3. Results and discussion

3.1. Properties of the MAILs

The obtained $C_n$mim/$FeCl_4$ MAILs were characterized by Raman spectroscopy, FTIR, ultraviolet and visible absorption spectrum, TGA and magnetic susceptibility. The MAILs represented a painted liquid with brown or green colors. The physical characterization was carried out by Raman spectroscopy (LabRAM HR-800) with the λ = 532 nm line from an air-cooled Nd:YAG laser at room temperature (~25 °C) under atmospheric pressure from raman shift 0 cm^{-1} to 3500 cm^{-1} with resolution 4 cm^{-1} overlay times 20 at laser power of 8 mW. The raman spectra of $C_n$mim/$FeCl_4$ are shown in Fig. 1. As shown in Fig. 1, the observed raman spectra of the $C_n$mim/$FeCl_4$ showed the very similar patterns as that of $C_n$mimCl, indicating that the $C_n$mim cation predominates. Those peaks at 332 cm^{-1} were reported and assigned very well to the symmetric

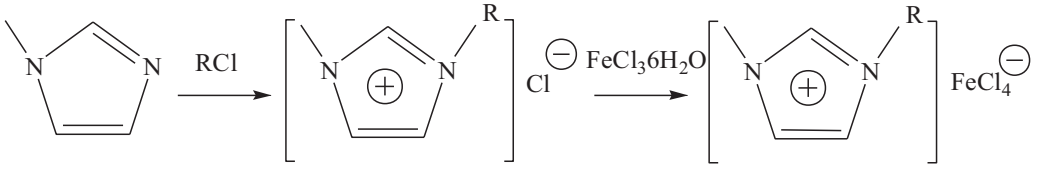

Scheme 2. Synthetic pathway of $C_n$mim/$FeCl_4$ MAILs (n = 4, 6, 8, 10, 12, 14, 16). 1. R=C_4H_9, 2. R=C_6H_{13}, 3. R=C_8H_{17}, 4. R=$C_{10}H_{21}$, 5. R=$C_{12}H_{25}$, 6. R=$C_{14}H_{29}$, 7. R=$C_{16}H_{33}$.

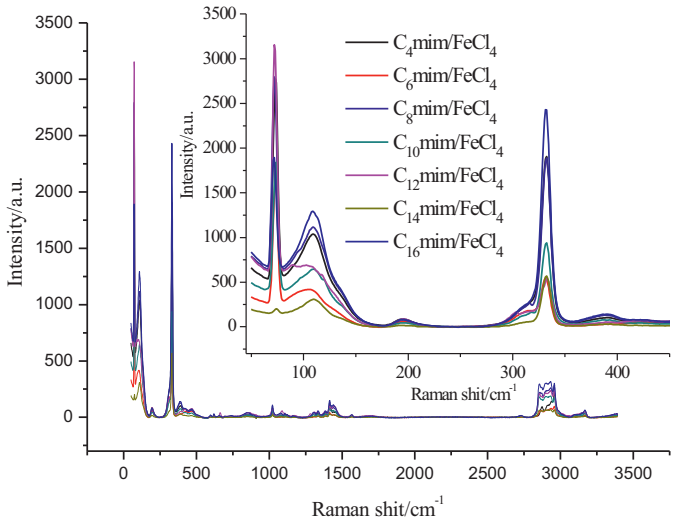

Fig. 1. Raman spectra of the synthetic $C_n$mim/$FeCl_4$ MAILs (n = 4, 6, 8, 10, 12, 14, 16).

Fe—Cl bond stretch vibrations of $[FeCl_4]^-$ in the literature (Lin & Vasam, 2005).

Finding $FeCl_4^{-1}$ in these liquids is not accidental and surprising, as it has been found as the primary Fe-containing compounds in basic chloroaluminate melts prepared with *N*-*n*-butypyridinium chloride. However, the peak observed at 72 cm^{-1} and 109 cm^{-1} does not correspond with a known $FeCl_4^-$ feature, and this feature may be due to the $C_n$mim cation. Thus, it can also be confirmed that the tested samples contain the same $[FeCl_4]^-$ anions (Wang et al., 2012).

Infrared spectra of imidazolium salts have revealed particular information about metal halide interactions through hydrogen bonding force. By comparing the FTIR spectra of $C_n$mim/$FeCl_4$ with each other (shown in Fig. 2), it can be seen that the spectra are quite similar to each other. From fingerprint area (400–1750 cm^{-1}) to characteristic frequency area (2500–4000 cm^{-1}), there are no differences except the sharper peaks arising from the complexes spectra. The stretching mode of the aromatic C—H bonds (C(2)-H, C(4)-H and C(5)-H) originate from the imidazolium ring structural features. The two higher frequency bands in the range of 3149–3151 cm^{-1} and 3110–3117 cm^{-1} are assigned to the stretching modes of C(4)-H or C(5)-H bond, the band assigned to the C(2)-H stretching mode appeared at lower frequency regions of 3093–3096 cm^{-1}. IR (KBr) of C_4mim/$FeCl_4$: 3097 m, 3112 s, 3145 s (C—H aromatic); 2963 m, 2933 s, 2876 s (C—H aliphatic) cm^{-1}. In all the examined MAILs exist absorption bands of imidazole ring ($\nu_{C=C\ ring} = \nu_{C-Harom}$ = 3100–31,501; for C_4mim/$FeCl_4$ $\nu_{as\ ring}$ = 1467, 1164; $\nu_{amide\ III}$ = 621 cm^{-1}). The analysis indicates that the $C_n$mim/$FeCl_4$ MAILs have similar cationic structures as the $C_n$mimCl and the anions of complexes have little effect on the chemical shifts of MAILs complexes.

The ultraviolet and visible absorption spectrum of $C_n$mim/$FeCl_4$ is shown in Fig. 3. The spectra resemble each other and show four characteristic bands of the [FeCl] ion at 227, 262, 327, and 354 nm (Friedman, 1952). The spectra in the ultraviolet and visible regions indicate the presence in the composition of MAILs of particle $[FeCl_4^-]$ in the form of the anion. Similar spectra for MAILs based on derivatives of imidazolium and $FeCl_3$ are presented in published data (Hayashi et al., 2006).

Moreover, the TGA shows that the sample does not lose weight when heated until 250 °C. Contrary to what was reported by Holbrey and Seddon (Holbrey & Seddon, 1999) that all the ILs samples underwent drying at 100 °C at pressure of 0.5 Torr, the

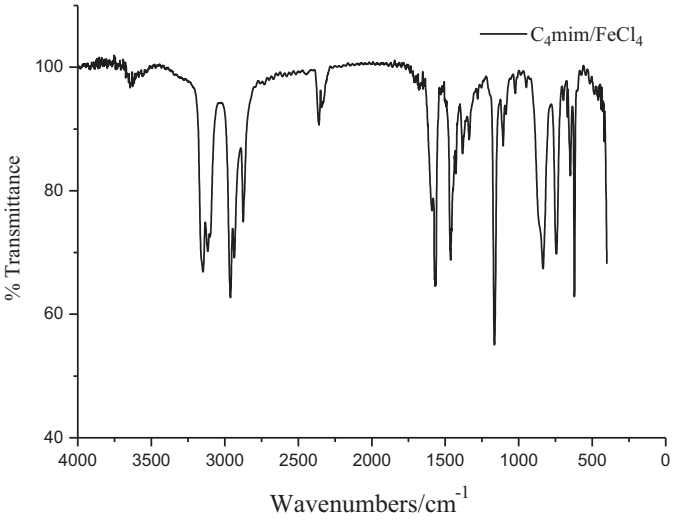

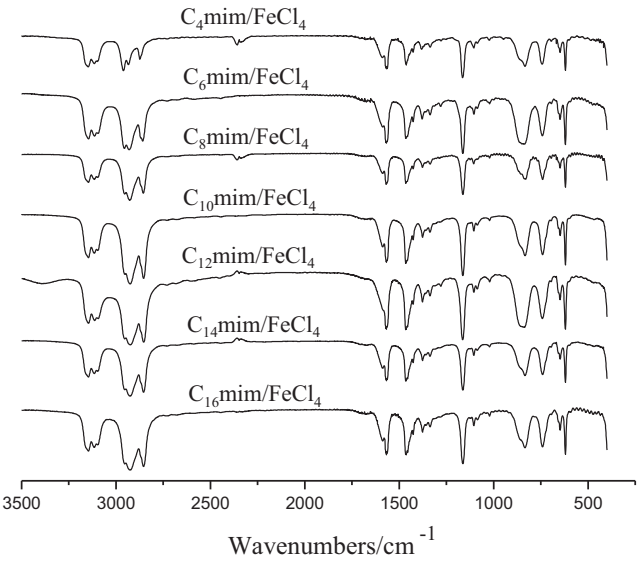

Fig. 2. FTIR spectra of the synthetic $C_n$mim/$FeCl_4$ MAILs (n = 4, 6, 8, 10, 12, 14, 16).

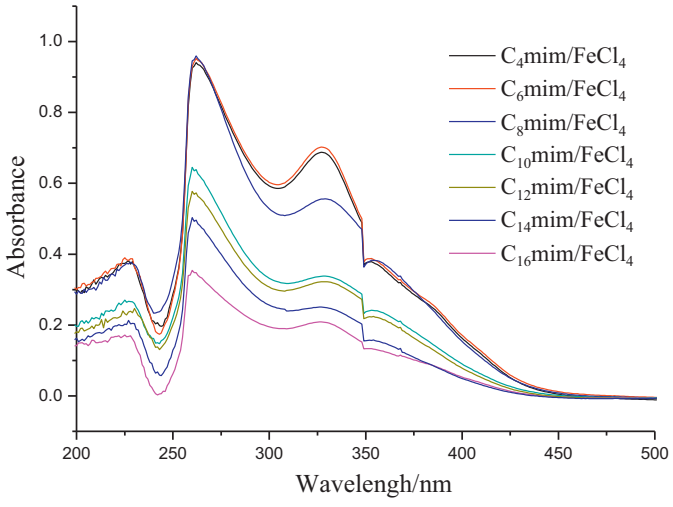

Fig. 3. Ultraviolet and visible absorption spectra of the synthetic $C_n$mim/$FeCl_4$ MAILs (n = 4, 6, 8, 10, 12, 14, 16).

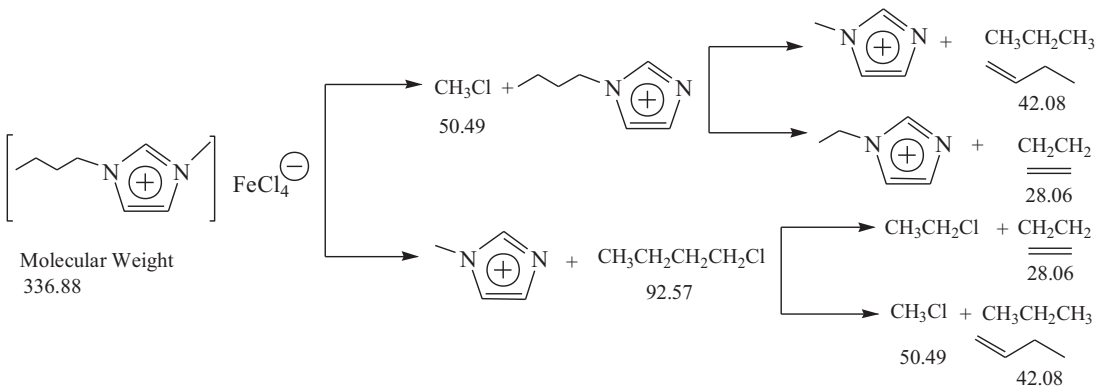

Scheme 3. Possible mechanism for the two steps decomposition of $C_n$mim/$FeCl_4$ MAILs (n = 4, 6, 8, 10, 12, 14, 16).

water content was calculated to be lower than 200 ppm. It can thus be considered that the synthetic ILs contain almost no free water (Song et al., 2010; Zhou et al., 2013c). The weight losses of $C_n$mim/$FeCl_4$ (n = 4, 6, 8, 10, 12, 14, 16) in a N_2 atmosphere occurring in the range of 250/310 °C (onset decomposition temperature, T_{onset}) to 480 °C varied from 62.01%, 60.61%, 64.14%, 66.64%, 72.86%, 66.29% and 66.38% (Fig. 4) respectively, due to the decomposition temperature (T_d). In the rapid decomposition process from 250 °C to T_d, the anions thermally decompose through dealkylation, whereas the cations mainly undergo alkyl migration and elimination reactions (Scheme 3). In the temperature range of 480–810 °C, the weight loss 11–17%; unburned residue 12–23% remains after 810 °C.

The magnetic susceptibilities of the MAILs were carried out by the MPMS (SQUID), and the results are shown in Fig. 5. A small amount of $C_n$mim/$FeCl_4$ (0.0030–0.0070 g) was enclosed in a capsule and measured at 293.15 K in the magnetic field range from -800 KA m^{-1} to 800 KA m^{-1}. It can be seen that magnetization intensities of the seven MAILs exhibit a hysteresis loop behavior in the magnetic field (Hao et al., 2010; Li et al., 2009). The hysteresis loop measurement was used to determine the magnetic parameters such as the specific saturation magnetization (M_s), coercivity (H_c) and remanence (M_r). The hysteresis loop for $C_n$mim/$FeCl_4$ is shown in Fig. 5. From the hysteresis loop, the $C_n$mim/$FeCl_4$ shows a typical hard-magnetic materials behavior, and the characteristics parameters are shown in Table 1.

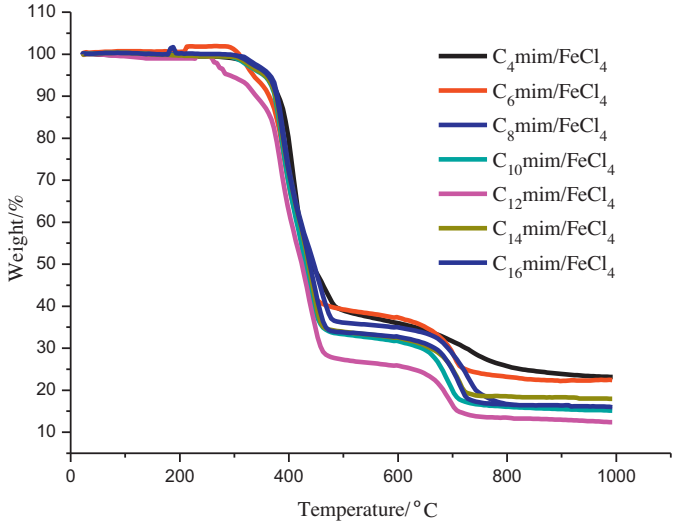

Fig. 4. TGA curves of the synthetic $C_n$mim/$FeCl_4$ MAILs in a nitrogen atmosphere (n = 4, 6, 8, 10, 12, 14, 16).

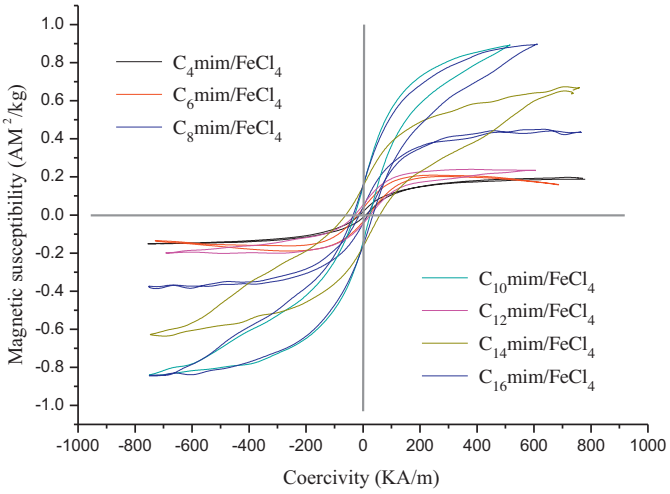

Fig. 5. Hysteresis loops of the synthetic $C_n$mim/$FeCl_4$ MAILs (n = 4, 6, 8, 10, 12, 14, 16).

3.2. Catalytic activity of the MAILs

We also present an attempt to adopt the DFT calculations to predict the reaction mechanism for glucose/xylose conversion to HMF catalyzed by $C_n$mim/MCl_3 complexes, and then to find out the dependence of the reactivity difference on various MCl_3 (M=W, Mo, Cr and Fe) in the same oxidation states. Scheme 1 shows the reaction mechanism of cellulose dissolved in $C_n$mim/MCl_4 and conversion of cellulose to HMF catalyzed with $C_n$mim/MCl_4. The trivalent Cr^{III}, Mo^{III} and W^{III} complexes were processed in high spin-state. The choice for the spin state was supported by previous works on Cr^{III} chlorides (Robertson et al., 2003). The Fe^{III}-containing complex was in line with a low spin-state. In addition, in the light of B3LYP energetics, the step related to the first water removal is the most different of the three steps dehydration, followed by the release of the second water, while the loss of the

Table 1
The magnetic susceptibilities of $C_n$mim/$FeCl_4$ MAILs at temperature 293.15 K (n = 4, 6, 8, 10, 12, 14, 16).

Compound	M_s/(AM²/kg)	H_c(KA/m)	M_r/(AM²/kg)	M_r/M_s
C_4mim/$FeCl_4$	0.19	8.1	0.018	0.095
C_6mim/$FeCl_4$	0.20	18.8	0.032	0.160
C_8mim/$FeCl_4$	0.44	16.2	0.042	0.095
C_{10}mim/$FeCl_4$	0.89	24.5	0.118	0.133
C_{12}mim/$FeCl_4$	0.23	25.7	0.050	0.217
C_{14}mim/$FeCl_4$	0.66	59.3	0.147	0.223
C_{16}mim/$FeCl_4$	0.90	36.2	0.167	0.186

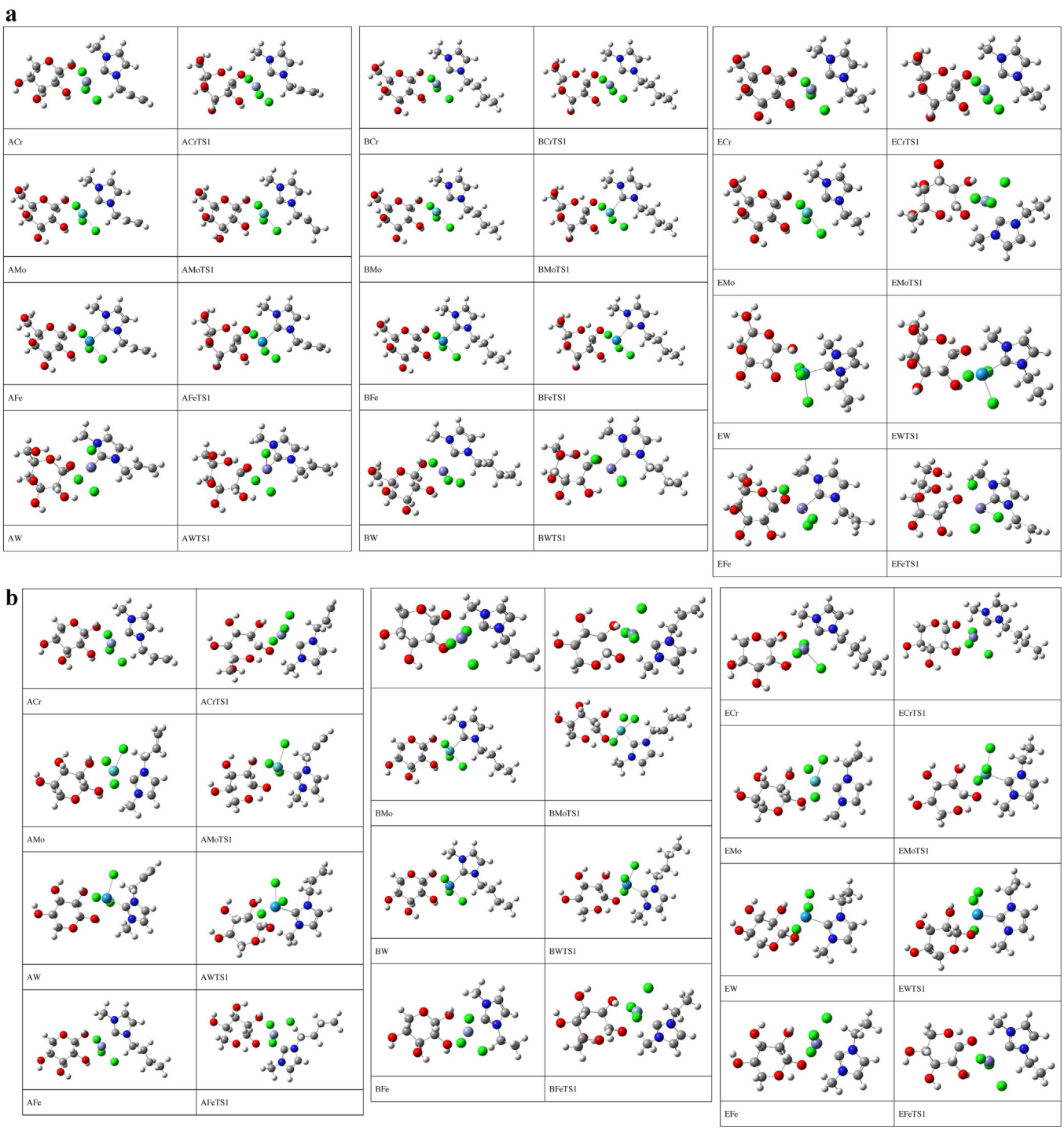

Fig. 6. The equilibrium and transition structure geometries of the optimized state on the reaction coordinate of glucose (a)/xylose (b) dehydrations to HMF catalyzed by $C_n$mim/MCl_3 (n = 2, 3, 4; M=Cr, Fe, Mo, W) complexes. C_2mim-E, C_3mim-A, C_4mim-B.

third water is considered to be the easiest step dehydration. Fig. 6 described the DFT-optimized structures of $CrCl_3$, $FeCl_3$, $MoCl_3$ and WCl_3 containing complexes involved in the dehydration at the first water removal. The change of Gibbs energy (△G) is determined at 293.15 K and the results are shown in Table 2. The Gibbs energy barriers at 293.15 K indicated that the reaction activities of the dehydration processes over different $C_n$mim/MCl_3 (n = 2, 3 and 4; M=W, Mo, Cr and Fe) active sites decrease in the order of C_3mim/WCl_3 > C_3mim/$CrCl_3$ > C_3mim/$MoCl_3$ > C_3mim/$FeCl_3$ for glucose and C_3mim/WCl_3 > C_3mim/$MoCl_3$ > C_3mim/$CrCl_3$ > C_3mim/$FeCl_3$ for xylose, respectively, in which C_3mim/WCl_3 may be the most promising catalyst. These preliminary calculations with DFT simulation are intrinsically more difficult to happen than actual using $CrCl_3$, $MoCl_3$ and WCl_3 catalysts put into practice. Accordingly, C_3mim/WCl_3 possesses the highest activities in the conversion of glucose/xylose to HMF and may be the most hopeful catalyst. It comes out that various intermediates and formations along with the reaction coordinate are predicted to be thermodynamically potential confirmed, in which the removal of the first water is the rate control step in the reaction,

Table 2
Gibbs energy of glucose/xylose dehydrations into HMF catalyzed by $C_n$mim/MCl_3 at 293.15 K (n = 2, 3, 4; M=Cr, Fe, Mo, W).

$C_n$mim/MCl_3	Gibbs energy (kcal/mol)	
	Glucose	Xylose
C_2mim/$CrCl_3$	46.42	43.87
C_2mim/$FeCl_3$	48.23	44.17
C_2mim/$MoCl_3$	44.86	43.31
C_2mim/WCl_3	44.45	42.70
C_3mim/$CrCl_3$	44.21	43.63
C_3mim/$FeCl_3$	46.01	43.78
C_3mim/$MoCl_3$	44.67	42.61
C_3mim/WCl_3	44.01	42.58
C_4mim/$CrCl_3$	46.41	44.45
C_4mim/$FeCl_3$	47.25	45.09
C_4mim/$MoCl_3$	44.75	42.93
C_4mim/WCl_3	44.31	42.66

while the release of the second and third waters can become easier.

4. Conclusions

The synthesized MAILs contained anion [$FeCl_4^-$] and various cations based on $C_n$mim$^+$. It was established that all synthesized MAILs were stable up to 250–310 °C. The decomposition was carried out in two steps with the formation of difficult decomposed residue (Scheme 3). The MAILs display a typical hard magnetic materials characteristic and with rather strong magnetic susceptibilities. The Gibbs energy barriers at 293.15 K indicated that C_3mim/WCl_3 may be the most active catalyst for breakage of glucosidic bonds and hydrolysis of glucose/xylose to HMF platform compound. As far as the advantages and potential application is concerned, the MAILs also have the potential to open up more promising new catalytic systems.

Acknowledgements

The authors would like to thank Dr Jonathan G. Heddle and Dr Ting-yu Lin, Advanced Science Institute, RIKEN, who gave valuable suggestions that have contribute to enhance the quality of the manuscript. The work was funded by National Natural Science Foundation of China (Nos. 31170672, 30940058), China Postdoctoral Science Foundation (2013M541621; 1302152C), Jiangsu Government Scholarship Fund for Study Abroad, the Foundation for the Eminent Talents and Research Foundation for Advanced Talents of Jiangsu University (12JDG074) and the Project Funded by the Priority Academic Program Development of Jiangsu Higher Education Institutions.

References

Bourissou, D., Guerret, O., Gabbai, F. P., & Bertrand, G. (2000). Stable carbenes. *Chemical Reviews*, *100*, 39–91.
Engel, P., Mladenov, R., Wulfhorst, H., Jäger, G., & Spiess, A. (2010). Point by point analysis: How ionic liquid affects the enzymatic hydrolysis of native and modified cellulose. *Green Chemistry*, *12*, 1959–1966.
Friedman, H. L. (1952). The visible and ultraviolet absorption. Spectrum of the tetrachloroferrate(III) ion in various media. *Journal of the American Chemical Society*, *74*, 5–10.
Friedlingstein, P., & Solomon, S. (2005). Contributions of past and present human generations to committed warming caused by carbon dioxide. *Proceedings of the National Academy of Sciences*, *102*, 10832–10836.
Godfray, H. C. J., Beddington, J. R., Crute, I. R., Haddad, L., Lawrence, D., Muir, J. F., et al. (2010). Food security: The challenge of feeding 9 billion people. *Science*, *327*, 812–818.
Hao, Y., Peng, J., Hu, S. W., Li, J. Q., & Zhai, M. L. (2010). Thermal decomposition of allyl-imidazolium-based ionic liquid studied by TGA–MS analysis and DFT calculations. *Thermochimica Acta*, *501*, 78–83.
Hatakeyama, T., Hashimoto, S., Ishizuka, K., & Nakamura, M. (2009). Highly selective biaryl cross-coupling reactions between aryl halides and aryl grignard reagents: A new catalyst combination of *N*-heterocyclic carbenes and iron, cobalt, and nickel fluorides. *Journal of the American Chemical Society*, *131*, 11949–11963.
Hay, P. J., & Wadt, W. R. (1985). Ab initio effective core potentials for molecular calculations. Potentials for K to Au including the outermost core orbitals. *Journal of Chemical Physics*, *82*, 299–310.
Hayashi, S., Saha, S., & Hamaguchi, H. (2006). A new class of magnetic fluids: bmim[$FeCl_4$] and nbmim[$FeCl_4$] ionic liquids. *IEEE Transactions on Magnetics*, *42*, 12–14.
Hu, S. Q., Zhang, Z. F., Song, J. L., Zhou, Y. X., & Han, B. X. (2009). Efficient conversion of glucose into 5-hydroxymethylfurfural catalyzed by a common Lewis acid $SnCl_4$ in an ionic liquid. *Green Chemistry*, *11*, 1746–1749.
Huang, Y. B., & Fu, Y. (2013). Hydrolysis of cellulose to glucose by solid acid catalysts. *Green Chemistry*, *15*, 1095–1111.
Kim, J. Y., Kim, J. T., Song, E. A., Min, Y. K., & Hamaguchi, H. O. (2008). Polypyrrole nanostruc-tures self-assembled in magnetic ionic liquid as a template. *Macromolecules*, *41*, 2886–2889.
Lange, J. P., Heide, E., Buijtenen, J., & Price, R. (2012). Furfural—A Promising platform for lignocellulosic biofuels. *ChemSusChem*, *5*, 150–166.
Lee, C., Yang, W., & Parr, G. (1988). Development of the colle-salvetti correlation-energy formula into a functional of the electron density. *Physical Review B*, *37*, 785–789.
Li, L., Huang, Y., Yan, G. P., Liu, F. J., Huang, Z. L., & Ma, Z. B. (2009). Poly (3, 4-ethylenedioxythiophene) nanospheres synthesized in magnetic ionic liquid. *Materials Letters*, *63*, 8–10.
Liang, Y., Zhou, H. L., & Yu, Z. X. (2009). Why is copper (I) complex more competent than dirhodium(II) complex in catalytic asymmetric OH insertion reactions? A computational study of the metal carbenoid OH insertion into water. *Journal of the American Chemical Society*, *131*, 17783–17785.
Lin, I. J. B., & Vasam, C. S. (2005). Metal containing ionic liquids and ionic liquid crystals based on imidazolium moiety. *Journal of Organometallic Chemistry*, *690*, 3498–3512.
Misuka, V., Breucha, D., & Löwe, H. (2011). Paramagnetic ionic liquids as "liquid fixed-bed" catalysts in flow application. *Chemical Engineering Journal*, *173*, 536–540.
Nel, W. P., & Cooper, C. J. (2009). Implications of fossil fuel constraints on economic growth and global warming. *Energy Policy*, *37*, 166–180.
Nishiyama, Y., Langan, P., & Chanzy, H. (2002). Crystal structure and hydrogen-bonding System in cellulose Iβ from synchrotron X-ray and neutron fiber diffraction. *Journal of the American Chemical Society*, *124*, 9074–9082.
Pei, X. W., Yan, Y. H., Yan, L. Y., Yang, P., Wang, J. L., Xu, R., et al. (2010). A magnetically responsive material of single-walled carbon nanotubes functionalized with magnetic ionic liquid. *Carbon*, *48*, 2501–2505.
Pidko, E. A., Degirmenci, V., van Santen, R. A., & Hensen, E. J. M. (2010). Glucose activation by transient. Cr^{+2} dimers. *Angewandte Chemie-International Edition*, *49*, 2530–2534.
Robertson, N. J., Carney, M. J., & Halfen, J. A. (2003). Chromium(II) and chromium(III) complexes supported by tris(2-pyridylmethyl)amine: Synthesis, structures, and reactivity. *Inorganic Chemistry*, *42*, 6876–6885.
Salvador, A. C., Santos, M. C., & Saraiva, J. A. (2010). Effect of the ionic liquid [bmim]Cl and high pressure on the activity of cellulose. *Green Chemistry*, *12*, 632–635.
Shafiee, S., & Topal, E. (2005). When will fossil fuel reserves be diminished? *Energy Policy*, *37*, 181–189.
Shimizu, K., & Satsum, A. (2011). Toward a rational control of solid acid catalysis for green synthesis and biomass conversion. *Energy and Environmental Science*, *4*, 3140–3153.
Torget, R. W., Kim, J. S., & Lee, Y. Y. (2000). Fundamental aspects of dilute acid hydrolysis/fractionation kinetics of hardwood carbohydrates. 1. cellulose hydrolysis. *Industrial and Engineering Chemistry Research*, *39*, 2817–2825.
Wang, H., Yan, R. Y., Li, Z. X., Zhang, X. P., & Zhang, S. J. (2011). Fe-containing magnetic ionic liquid as an effective catalyst for the glycolysis of poly(ethylene terephthalate). *Catalysis Communications*, *11*, 763–767.
Wang, M., Li, B., Zhao, C. J., Qian, X. Z., Xu, Y. L., Chen, G. R., et al. (2010). Recovery of [BMIM] $FeCl_4$ from homogeneous mixture using a simple chemical method. *Korean Journal of Chemical Engineering*, *27*, 1275–1277.
Xu, J., Chen, H., Z, Kádár, Thomsen, Z., Schmidt, A. B., Peng, J. E., & H. (2011). Optimization of microwave pretreatment on wheat straw for ethanol production. *Biomass and Bioenergy*, *35*, 3859–3864.
Wang, J., Yao, H., Nie, Y., Zhang, X., & Li, J. (2012). Synthesis and characterization of the iron-containing magnetic ionic liquids. *Journal of Molecular Liquids*, *169*, 152–155.
Holbrey, J. D., & Seddon, K. R. (1999). Ionic liquids. *Journal of Cleaner Production*, *1*, 223–236.
Song, F., Shen, X., Liu, M., & Xiang, J. (2010). Formation and characterization of magnetic barium ferrite hollow fibers with high specific surface area via sol–gel process. *Solid State Sciences*, *12*, 1603–1607.
Zakzeski, J., Bruijnincx, P. C. A., Jongerius, A. L., & Weckhuysen, B. M. (2010). The catalytic valorization of lignin for the production of renewable chemicals. *Chemical Review*, *110*, 3552–3599.
Zhao, H., Holladay, J., Brown, H., & Zhang, Z. C. (2007). Metal chlorides in ionic liquid solvents convert sugars to 5-hydroxymethylfurfural. *Science*, *316*, 1597–1600.
Zhou, C., Yu, X., Ma, H., He, R., & Vittayapadung, S. (2013). Optimization on the conversion of bamboo shoot shell to levulinic acid with environmentally benign

acidic ionic liquid and response surface analysis. *Chinese Journal of Chemical Engineering*, *21*, 544–550.

Zhou, C., Yu, X., Ma, H., Zhang, Z., Lin, L., Yagoub, A., et al. (2013). Solid–liquid extraction kinetics of flavonoids from okra (*Abelmoschus esculentus* L. Moench) pods with applicability analysis. *Advanced Materials Research*, *750*, 1560–1566.

Zhou, C., Yu, X., Yang, H., Zhang, Y., Wang, Y., Lin, L., et al. (2013). Preparation of levulinic acid by acid-catalysed hydrolysis of bamboo shoot shell in the presence of acidic ionic liquid using Box–Behnken design. *Energy Sources Part A*, *35*, 1852–1862.